Available online at www.sciencedirect.com

ScienceDirect

Virology 360 (2007) 92–104

VIROLOGY

www.elsevier.com/locate/yviro

Double-labelled HIV-1 particles for study of virus–cell interaction

Marko Lampe [a], John A.G. Briggs [b], Thomas Endress [b], Bärbel Glass [a], Stefan Riegelsberger [b], Hans-Georg Kräusslich [a], Don C. Lamb [c,d,b], Christoph Bräuchle [c,b], Barbara Müller [a,*]

[a] *Department of Virology, Universitätsklinikum Heidelberg, Im Neuenheimer Feld 324, 69120 Heidelberg, Germany*
[b] *Department of Chemistry and Biochemistry, Ludwig-Maximilians-Universität München, Butenandtstr. 11, Haus E, 81377 Munich, Germany*
[c] *Center for NanoScience, Ludwig-Maximilians-Universität München, Geschwister-Scholl-Platz 1, 80539 Munich, Germany*
[d] *Department of Physics, University of Illinois at Urbana-Champaign, Urbana, IL 61801, USA*

Received 24 July 2006; returned to author for revision 19 September 2006; accepted 3 October 2006
Available online 9 November 2006

Abstract

Human immunodeficiency virus (HIV) delivers its genome to a host cell through fusion of the viral envelope with a cellular membrane. While the viral and cellular proteins involved in entry have been analyzed in detail, the dynamics of virus–cell fusion are largely unknown. Single virus tracing (SVT) provides the unique opportunity to visualize viral particles in real time allowing direct observation of the dynamics of this stochastic process. For this purpose, we developed a double-coloured HIV derivative carrying a green fluorescent label attached to the viral matrix protein combined with a red label fused to the viral Vpr protein designed to distinguish between complete virions and subviral particles lacking MA after membrane fusion. We present here a detailed characterization of this novel tool together with exemplary live cell imaging studies, demonstrating its suitability for real-time analyses of HIV–cell interaction.

Keywords: HIV-1; Single virus tracing; Virus entry; Fluorescence labelling; Heparan sulfate

Introduction

Entry of enveloped viruses and delivery of their genome into a susceptible cell starts by fusion of the viral lipid envelope with a cellular membrane. Fusion can take place either at the plasma membrane or at intracellular membranes, most notably those of the endosomal pathway, and both strategies are used by different viruses (for review, see Eckert and Kim, 2001; Sieczkarski and Whittaker, 2005). While the cellular attachment molecules, receptors and coreceptors, and the viral surface molecules mediating entry are known for many viruses and have been analyzed in detail, there is currently little information available concerning the dynamics of viral entry. This is mainly due to the fact that bulk biochemical models can yield only limited information on the kinetics of this stochastic process and suitable methods for tracking individual virus entry events with high temporal and spatial resolution have been lacking.

Recently, biophysical imaging techniques allowing observation of individual fluorescently labelled molecules or particles in living cells have become available. Such methods are ideally suited for the analysis of dynamic events involved in virus–cell interactions. They have been applied to investigate the entry processes of the non-enveloped viruses adeno-associated virus (AAV; Seisenberger et al., 2001), adenovirus (Suomalainen et al., 1999), SV40 (Damm et al., 2005) and polyomavirus (Ewers et al., 2005), as well as of the enveloped viruses influenza virus (Lakadamyali et al., 2003; Rust et al., 2004), rabies virus (Finke et al., 2004) and murine leukemia virus (Lehmann et al., 2005). Having previously established a method for single virus tracing (SVT) based on wide-field imaging, which allows direct observation of fluorescently labelled AAV virions in real time with single molecule sensitivity (Seisenberger et al., 2001; Bräuchle et al., 2002), we wanted to adapt this technique to study the entry process of human immunodeficiency virus type 1 (HIV-1).

Previous studies on HIV fusion dynamics have mainly employed bulk measurements using cell–cell fusion assays (see Gallo et al., 2003, for review) and indirect readout methods to

* Corresponding author. Fax: +49 6221 565003.
E-mail address: Barbara_Mueller@med.uni-heidelberg.de (B. Müller).

0042-6822/$ - see front matter © 2006 Elsevier Inc. All rights reserved.
doi:10.1016/j.virol.2006.10.005

monitor fusion. In studies investigating particle–cell fusion, entry events were synchronized through pre-binding and temperature shift (Raviv et al., 2002; Markosyan et al., 2005). In contrast, SVT using fluorescently labelled virus derivatives allows direct analysis of fast steps in the interaction of individual particles with host cells in tissue culture at 37 °C. A prerequisite for the application of this technique is the introduction of an appropriate fluorescent label into the virion. In the case of HIV, a labelling strategy which allows discrimination between complete particles and subviral complexes would be highly advantageous. It has long been established that productive HIV entry can occur by direct fusion at the plasma membrane, mediated by interaction of the viral surface glycoprotein with the cellular receptor CD4 and co-receptor molecules, but productive entry of HIV particles through an endocytic pathway and pH-independent fusion has also been observed (Daecke et al., 2005). In analyses of individual cell entry events by SVT it is thus crucial to discriminate between fusion at the plasma membrane and uptake of complete particles by endocytosis. Towards this end, we have combined our previously described HIV-1 derivative, which carries an enhanced GFP (eGFP) domain attached to the membrane bound matrix (MA) region of the HIV structural protein Gag (Müller et al., 2004), with an mRFP1-labelled Vpr derivative. Fluorescent labelling of the virion incorporated protein Vpr has been used previously to follow the intracellular trafficking of viral pre-integration complexes after fusion (McDonald et al., 2002). The novel dual-labelling strategy described here should allow distinguishing intact double-coloured viruses from single-coloured subviral particles resulting from membrane fusion. As an essential prerequisite for the suitability of double-labelled HIV for studies on virus–cell interaction, we have carried out a detailed analysis on the functionality and fluorescence characteristics of the labelled HIV particles under conditions suitable for live cell imaging.

Results and discussion

Characterization of double-labelled infectious HIV-1 particles

We had previously generated an infectious fluorescently labelled HIV-1 derivative carrying eGFP attached to the membrane bound MA domain of the main HIV-1 structural protein Gag as a tool for studying the dynamics of HIV–cell interaction. Cells transfected with this plasmid released fluorescently labelled particles. Mixed particles generated by co-transfection with an equimolar amount of wild-type genomes retained full infectivity while carrying an average of approximately 2500 molecules of eGFP (Müller et al., 2004). Initial microscopic studies aimed at investigating the interaction of fluorescently labelled particles with cells revealed very efficient binding of these particles to CD4-positive HeLaP4 cells (data not shown). It remained unclear, however, whether bound particles subsequently underwent fusion or remained as complete particles at the membrane. Accordingly, single labelled particles did not appear suitable for the study of HIV-1 entry kinetics. We therefore decided to establish a double-labelling strategy in which the fluorescent label at the viral MA protein was combined with a differently coloured fluorescent protein fused to the viral protein Vpr. Exogenously expressed Vpr.eGFP had previously been shown to be incorporated into viral particles and was used to follow trafficking of viral replication complexes after cell entry (McDonald et al., 2002). Vpr is believed to largely remain with the viral replication and pre-integration complexes after fusion. In contrast, the vast majority of the membrane-attached MA molecules is expected to separate from the core immediately after membrane removal. Using double-labelling of HIV-1 particles in MA and Vpr, we should thus be able to distinguish extra- and intracellular double-labelled complete particles from single-labelled subviral complexes that have lost the MA layer. Initial investigations established that a combination of eGFP and monomeric red fluorescent protein (mRFP1) displayed better spectral separation and less photobleaching than the combination of cyan and yellow fluorescent proteins (data not shown). Hence, a combination of MA.eGFP and mRFP.Vpr was used in all subsequent experiments involving fluorescently double-labelled virions.

Our first aim was to determine whether such double-labelled HIV-1 particles could be generated efficiently and whether they retained infectivity. Previously, we observed that particles containing an equimolar mixture of native and eGFP-labelled Gag exhibited wild-type infectivity, while particles made only from Gag.eGFP were significantly less infectious (Müller et al., 2004). We therefore produced double-labelled particles by transfection of 293T cells with a 1:1 mixture of HIV-1 proviral DNA and its eGFP-tagged derivative together with a plasmid encoding the mRFP.Vpr fusion protein. Wild-type HIV-1, as well as single-labelled particles carrying only one of the two fluorescent fusion proteins, were generated in parallel.

To analyze whether viruses containing the modified proteins displayed normal protein composition and Gag processing, particles were centrifuged through a sucrose cushion and their protein composition was analyzed by immunoblotting using antisera against different HIV-1 proteins (Fig. 1A). Staining with antiserum against MA revealed that the MA.eGFP-labelled particles (lanes 2 and 3) contained comparable amounts of wild-type and eGFP-tagged Gag and MA. The fusion proteins were also detected using an antibody against eGFP (data not shown). In the presence of exogenously expressed mRFP.Vpr (lanes 3 and 4) Gag processing appeared to be impaired (compare lanes 1 and 4, as well as 2 and 3, respectively; see also below). Immunoblotting using αgp120 showed that comparable amounts of Env were incorporated in all cases. Antiserum against Vpr revealed virion incorporation of the mRFP.Vpr fusion protein with an apparent molecular mass of 38 kDa as well as wild-type Vpr produced from the proviral plasmids (migrating at 14 kDa). A smaller amount of an anti-Vpr reactive protein of approximately 30 kDa was also detected, presumably representing a product of internal proteolysis within mRFP1. The exogenously expressed mRFP.Vpr gave a much stronger band than the native Vpr indicating that over-expression of the fusion protein leads to increased virion incorporation. We had previously determined Vpr in wild-type HIV_{NL4-3} to be present

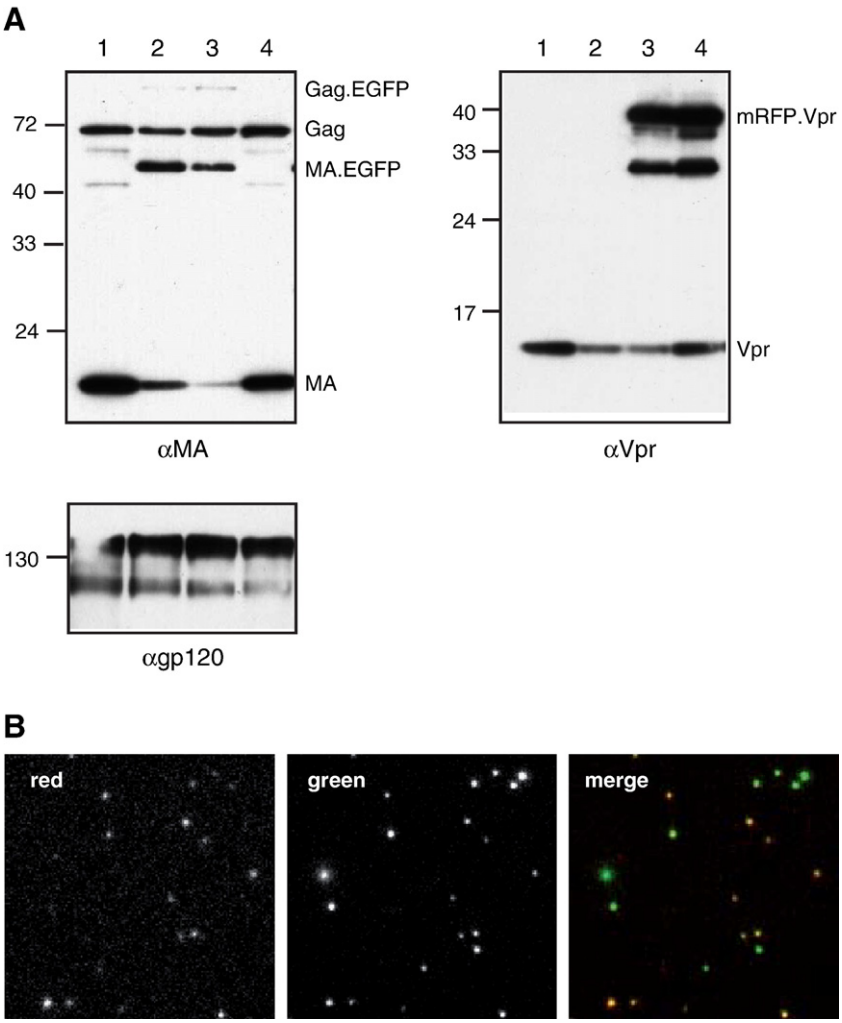

Fig. 1. Characterization of double-labelled virions. (A) Virus particles were prepared from the tissue culture supernatant of 293T cells transfected with proviral plasmid pNLC4-3 (lane 1), pNLC4-3 and pNLC4-3.eGFP (lane 2), pNLC4-3, pNLC4-3.eGFP and pmRFP.Vpr (lane 3) or pNLC4-3 and pmRFP.Vpr (lane 4), respectively. Following particle concentration through a sucrose cushion, viral proteins were separated by SDS–PAGE and detected by immunoblotting using polyclonal antisera raised against HIV-1 MA, Vpr or gp120 respectively. Positions of molecular weight standards in kDa are indicated to the left. The minor differences in gp120 incorporation were not reproducible when performing immunoblots using particle preparations from three independent experiments. (B) Virions prepared as in panel A were visualized by fluorescence microscopy using the experimental setup described in Materials and methods.

at a ratio of approximately1:7 to Gag (Müller et al., 2000), which corresponds to approximately 700 molecules, based on an average of 4900 molecules of Gag per particle (Briggs et al., 2004). Thus, over-expression of mRFP.Vpr led to the incorporation of far more than 1000 molecules of labelled Vpr per particle. Imaging of particles produced by this triple co-transfection showed that the vast majority of signals was dual-coloured confirming that both labels were contained within the same particles (Fig. 1B; see also below).

Relative infectivities of single- and double-labelled viruses were determined by titration of tissue culture supernatants from co-transfected cells on TZM reporter cells, which express luciferase under the control of the HIV-1 LTR (Wei et al., 2002). Infection leads to Tat-stimulated luciferase expression, which can be quantitated by a luminometric assay. The results from one such experiment are shown in Fig. 2. Infectivity was mildly reduced in the case of single labelling of either MA or Vpr,

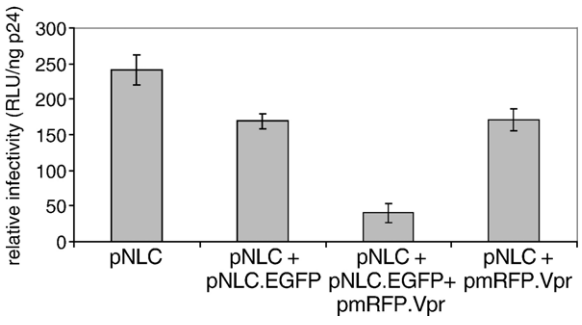

Fig. 2. Relative infectivity of fluorescently labelled VLPs. Particles obtained by co-transfection of 293T cells with the indicated plasmids were quantitated by p24 ELISA and titrated in triplicate on TZM reporter cells. At 48 hpi, infected cells were quantitated by luminescence measurements as described in Materials and methods and relative light units (RLU) per ng p24 were calculated. The figure shows data from one representative experiment. Two additional independent titrations yielded similar data.

while the combination of both labels had a more pronounced effect. In this case, the luminescence signal per input antigen (as determined by p24 ELISA) was reduced approximately fivefold compared to wild-type HIV-1. This effect is most likely due to the reduced Gag polyprotein processing in the presence of both fluorophores (Fig. 1A), and may result from molecular crowding in virus particles carrying a large number of fluorescent protein domains in addition to the viral structural proteins. Importantly, however, double-labelled particles retained significant infectivity and this approach therefore appeared suitable for SVT.

Preparation of double-labelled replication-defective HIV-1 variants for live cell imaging

For live-cell imaging experiments, it is desirable to use replication-defective HIV-1 derivatives that can be investigated in biosafety level 1 laboratories. We had previously used an HIV-1 expression plasmid (pKHIV), which produces all viral proteins except Nef and is fully entry-competent, but does not support a complete replication cycle, due to lack of the viral LTR sequences (Müller et al., 2004). Attempts to purify double-labelled particles from cells co-transfected with pKHIV derivatives and pmRFP.Vpr were not successful, however. Even low amounts of the mRFP.Vpr plasmid strongly reduced expression from pKHIV, resulting in extremely low particle release. This problem could be overcome by transferring the complete HIV-1-derived coding sequence into the mammalian expression vector pcDNA3.1 capable of episomal replication in 293T cells. The resulting plasmids pCHIV and pCHIV.eGFP allowed efficient co-expression together with mRFP.Vpr.

Double-labelled particles were generated by co-transfection of pCHIV derivatives and pmRFP.Vpr into 293T cells, harvested from the tissue culture supernatant and concentrated by centrifugation through a sucrose cushion. Immunoblot and fluorescence microscopy analysis of such particles yielded similar results as obtained for the infectious virus preparations. Since the presence of mRFP.Vpr had appeared to affect Gag processing (Fig. 1A), the optimal amount of mRFP.Vpr was defined by titration experiments. As shown in Fig. 3A, the relative amount of exogenously expressed mRFP.Vpr incorporated into particles correlated with the amount of expression plasmid transfected. Whereas a maximum amount of mRFP.Vpr per particle is desirable for optimal detection in real-time imaging, increased mRFP.Vpr incorporation resulted in decreased Gag processing efficiency and compromised HIV protein expression and particle release (Fig. 3A). If Vpr incorporation would be limited by molecular crowding, this may be overcome by decreasing the relative amount of Gag.eGFP per particle. Fig. 3B shows, however, that changing the ratio of wt Gag to Gag.eGFP from 1:1 to 1:4, while keeping the total ratio of Gag to Vpr constant, did not lead to increased mRFP.Vpr incorporation and did not alter Gag processing (Fig. 3B). Based on these results and microscopic evaluation of the respective particle preparations (not shown), a molar ratio of 1:1:0.4 (pCHIV:pCHIVeGFP:pmRFP.Vpr) was determined

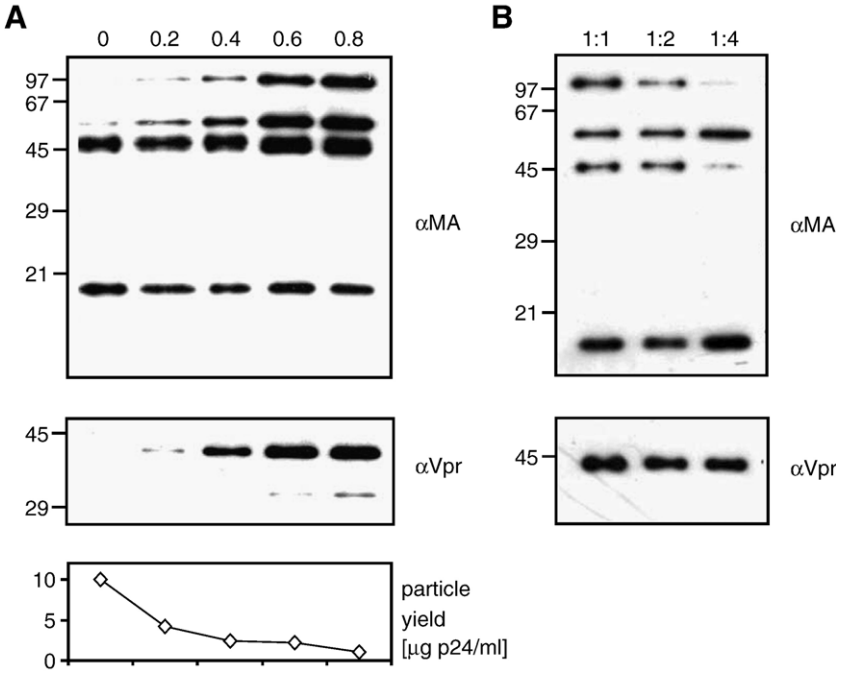

Fig. 3. Variation of labelling intensities. (A) Increasing the relative amount of Vpr. VLPs were prepared from the tissue culture supernatant of 293T cells transfected with increasing amounts of pmRFP.Vpr relative to HIV-derived plasmids. Numbers above the lanes indicate the relative amount of pmRFP.Vpr co-transfected to a constant amount of an equimolar mixture between pCHIV and pCHIV^{eGFP} (set to 1.0). Equivalent amounts of particles, as determined by p24 ELISA, were separated by SDS–PAGE and analyzed by immunoblotting using the indicated antisera. Particle yield was determined by ELISA quantitation of p24 CA. (B) Changing the relative amount of Gag.eGFP. Cells were co-transfected with the indicated ratios of wild-type versus eGFP-labelled pCHIV, while the total amount of pCHIV-derivatives and the relative amount of pmRFP.Vpr was kept constant (1.0 pCHIV derivatives: 0.2 pmRFP.Vpr). Particles were analyzed by immunoblotting as in panel A. Positions of molecular weight standards (in kDa) are indicated to the left.

to yield the optimal balance between labelling efficiency and mature particle production and was therefore used in all subsequent experiments.

Characterization of double-labelling efficiency

Discrimination between complete particles and subviral complexes based on the colour of the signal depends on a high degree of double-labelling. To quantitate the labelling efficiency, concentrated particles were adhered to glass coverslips and visualized at the conditions subsequently used for single virus tracing (Fig. 4A). Integrated fluorescence intensities of individual signals were quantitated using an automated data analysis routine. Fig. 4B displays eGFP and mRFP signal intensities from a representative preparation, each data point corresponding to an individual particle ($n=516$). The eGFP and mRFP intensity distributions for labelled particles are fairly broad. This variability is expected since HIV-1 particles display a flexible architecture with a broad range of diameters and are composed of variable amounts of Gag polyproteins (Wilk et al., 2001; Briggs et al., 2003, 2004). Most likely, it is this structural flexibility that allows the insertion of the relatively large eGFP domain into Gag without disrupting particle formation. A contribution of slightly uneven ratios of MA.eGFP:MA in different particles to the varying signal intensity cannot be excluded; however, a particle preparation lacking the unlabelled MA variant displayed an even broader distribution in eGFP intensities (data not shown). Variation in mRFP intensities was also expected because the number of Vpr molecules incorporated per particle is variable, depending on e.g. the expression efficiency in the host cell. Fig. 4B shows a rough correlation between the red and green fluorescence intensities of individual particles. This indicates that particles containing more MA.eGFP – presumably larger particles – also contained more mRFP.Vpr.

Given the wide variability in the eGFP and mRFP intensities, distinguishing single-labelled from double-labelled particles becomes a question of detection efficiency. For purpose of quantification, a value of one standard deviation above the background intensity was chosen as the minimum detection level. These levels are shown as lines in Fig. 4B. Particles to the left of the vertical line are considered red only and particles below the horizontal line are considered green only. Using these criteria, 92% of the particles were determined to be double-labelled, whereas 6.2% displayed only a green signal (MA) and 1.4% were found positive for the red signal (Vpr) only. The number of single-coloured particles determined using the method above represents an upper estimate as single-coloured signals corresponding to protein aggregates from broken particles would also be included in the evaluation. This could be confirmed using a preparation lacking wild-type Gag, which also displayed ~1% of mRFP.Vpr-only signals (data not shown). Since only labelled Gag was present, the red-only signal could not correspond to complete single-labelled particles. Microscopic analysis of a mock particle preparation from cells expressing only mRFP.Vpr on the other hand did not reveal any fluorescent signals indicating that mRFP.Vpr is not released from cells in the absence of particle production (data

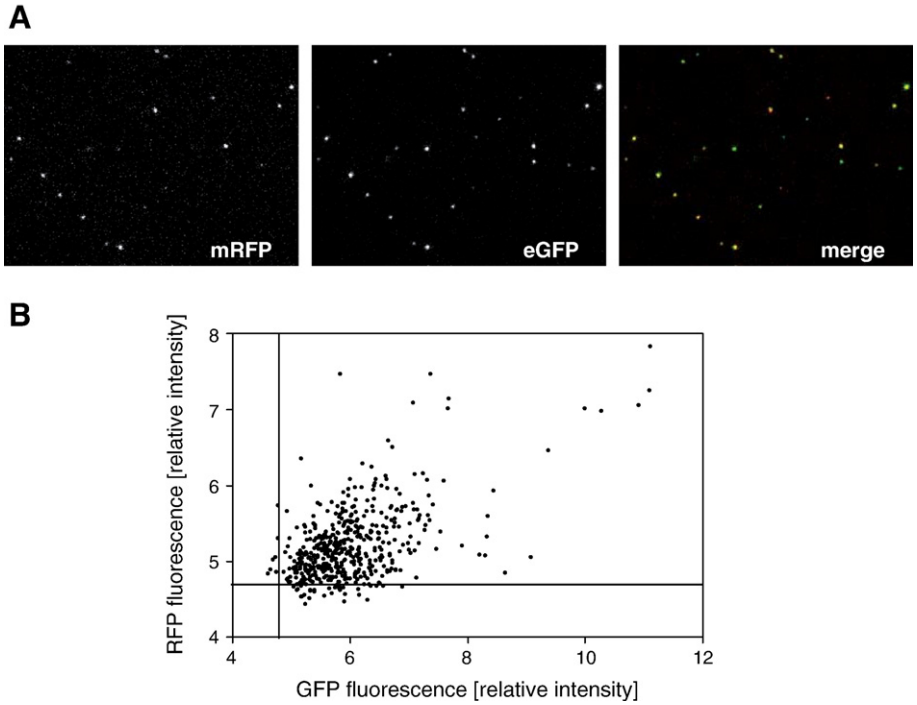

Fig. 4. Quantitation of double-labelling efficiency. (A) Particles were adhered to glass coverslips and visualized. Microscope settings were identical to those used for live cell imaging. (B) The integrated eGFP and mRFP1 fluorescence intensities of single particles adhered to a glass coverslip were determined as described in Materials and methods and plotted in arbitrary fluorescence units (values on the *x* and *y* axis correspond to integrated pixel intensities determined, divided by 100,000). Lines indicate the threshold as specified in Materials and methods. Particles displaying signal intensities above the threshold in both channels (upper right quadrant) were counted as double labelled.

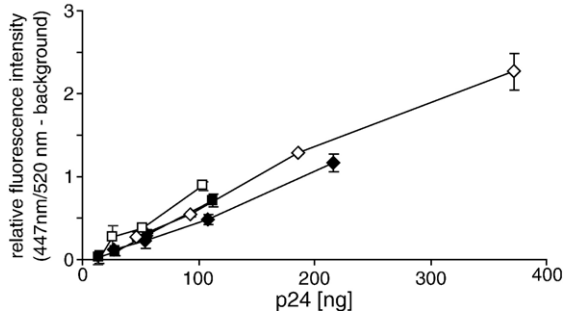

Fig. 5. Entry competence of fluorescently labelled particles. VLPs carrying the Vpr.BlaM reporter protein were prepared from 293T cells co-transfected with pCHIV and pMM310 expression plasmid (open symbols) or pCHIV, pCHIV.eGFP and pMM310 (filled symbols), respectively. Particles pelleted from the supernatant were quantitated by p24 ELISA, titrated in triplicate on HeLaP4 cells and fusion efficiency was analyzed as described in Materials and methods. Mean values of triplicates are plotted. Squares and diamonds represent values from two experiments using independent VLP preparations.

not shown). Since quantification of several independent particle preparations revealed some variation in relative double-labelling efficiencies between preparations, an analysis of double-labelling efficiency needs to be performed as a routine quality control for each particle preparation to be used in live cell imaging experiments.

Entry competence of fluorescently labelled particles

To determine the suitability of the fluorescently labelled, replication-defective particles for live cell imaging, we analyzed their fusion efficiency using a quantitative entry assay. This assay makes use of the incorporation of a Vpr-β-lactamase fusion protein (Vpr.BlaM) into particles. Enzymatically active BlaM is released into the cytoplasm upon fusion and can be quantitated by determining cleavage of the fluorescent substrate CCF2 (Cavrois et al., 2002; Münk et al., 2002). Although the Vpr.BlaM fusion protein is clearly not identical to the mRFP. Vpr fusion protein, we used this assay as a model system to compare the entry efficiency of MA.eGFP-labelled particles carrying an exogenously expressed Vpr fusion protein with their wild-type MA counterparts. Particles were titrated in parallel on HeLaP4 cells and fusion efficiency was quantitated by determining CCF2 cleavage. The result was similar for particles containing or lacking Gag.eGFP over a wide concentration range, indicating that the presence of MA.eGFP did not significantly affect the fusogenicity of particles (Fig. 5). We conclude that the presence of the MA.eGFP in VLPs does not significantly alter their fusion competence and MA.eGFP-labelled particles are suited for the real-time imaging of entry kinetics.

Tracing of individual fluorescent particles in real time

To determine the suitability of the double-fluorescent particles for live cell imaging of HIV-1 host cell interactions, we performed exemplary experiments on HeLaP4 cells. Double-labelled particles were added at a concentration similar to that used in the infection assays (25–100 ng p24/10^4 cells) and followed with a time resolution of 50 ms per frame. This gives a total time resolution per double-colour exposure of 100 ms since the excitation wavelength was alternated with each frame. Using the microscope setup described in Materials and methods, double-labelled particles were easily detected and traced under these conditions. Four different classes of events were observed and are summarized in Fig. 6 (movies displaying the indicated traces are provided as supplementary material). (i) Double-labelled, complete particles were detected in free diffusion between cells (Fig. 6, trace type a); (ii) complete, extracellular particles briefly touched the cell surface for a duration of 1–2 frames (<200 ms), before resuming free diffusion (Fig. 6, trace type b); (iii) double-labelled particles became immobile at the membrane immediately after cell contact (Fig. 6, trace type c); and (iv) double-labelled as well as some single-labelled particles displayed intracellular movement (Fig. 6, trace type d). Immobilization of double-labelled particles at the plasma membrane (trace type c) was a frequent event with most of these particles remaining immobile and double-coloured during the observation period. The majority of immobilized particles stayed double-labelled, even when the observation period was extended at lower temporal resolution to over 2 h at 37 °C, indicating that membrane fusion did not occur (data not shown). Accordingly, such particles accumulated at

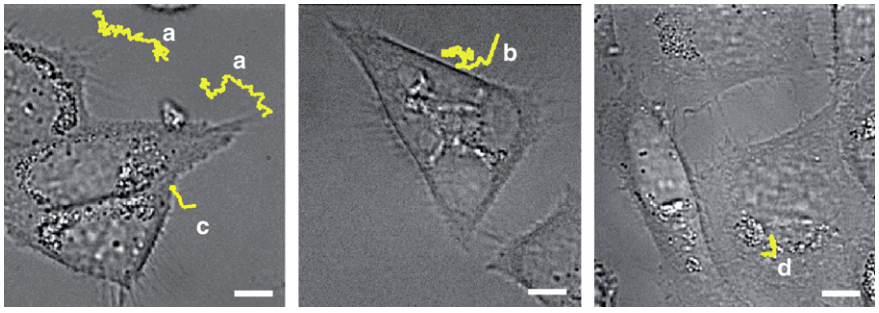

Fig. 6. Different types of virus–cell interactions observed in live cell imaging experiments. HeLaP4 cells were incubated with double-labelled particles at 37 °C and images were recorded at a time resolution of 100 ms per overlay image as described in Materials and methods. Exemplary traces of double-labelled particles are shown superimposed on a bright light image of cells. Free diffusion of double-labelled particles (trace type a), brief touches of the cell surface (trace type b), immobilization of particles at the cell membrane (trace type c), as well as intracellular movement of double-labelled (trace type d) or single-labelled particles were observed. Scale bar: 4 μm. Corresponding movies are provided as supplementary material.

the plasma membrane over time. These results indicate that immobilization of complete particles represents largely unproductive virus attachment (see also below).

The majority of fluorescent signals displaying intracellular movement were dual-coloured (Fig. 6, trace type d and supplementary material), indicating uptake of complete particles. This is in accordance with the fact that endocytosis of HIV particles can be readily observed in various cell types. Intracellular particles were most readily observed at time points greater than 10 min after fluorescent particle addition. Some complete particles displaying intracellular movement could already be detected at the earliest possible observation times after particle addition (~1 min), indicating very rapid endocytotic events. Besides double-labelled particles, we also observed some single-labelled signals undergoing directed movement within the cell, while no actual colour separation event was seen among >7000 particle traces observed. This was also the case when the HeLa derivative JC53, which had been selected for a particularly high surface expression of CD4 (Platt et al., 1998), was used in similar experiments (data not shown). The detection of intracellular particles carrying only the mRFP.Vpr label suggested that membrane fusion had occurred. This conclusion is not unequivocal, however, since the fluorescent particle preparations contained a low percentage of single-coloured signals (Fig. 4), which cannot be distinguished from subviral particles after fusion. It should be emphasized that this also holds true for previous studies tracing fluorescent Vpr complexes (McDonald et al., 2002). This limitation can only be overcome if the descent of an individual single-coloured signal from a double-labelled particle can be ascertained by observing the actual entry event (as colour separation) within the window of observation.

Observation of bulk colour separation

In the absence of observation of individual fusion events in the experiments described above, we aimed to verify that fusion would lead to a separation of colours. For this, we generated double fluorescently labelled pseudotyped particles, in which the HIV-1 envelope protein was replaced by the glycoprotein G from vesicular stomatitis virus (VSV-G), which mediates highly efficient entry into HeLaP4 cells. Unlike HIV-1 entry, VSV-G mediated uptake occurs through endocytosis followed by pH-triggered fusion with the endosomal membrane and can be blocked by bafilomycin A (Matlin et al., 1982; Palokangas et al., 1994). As expected, incubation of HeLaP4 cells with pseudotyped particles resulted in rapid intracellular accumulation of double-labelled particles. Upon prolonged incubation, we observed the appearance of a diffuse MA.eGFP signal in the cytoplasm, while an increased mRFP.Vpr signal was detected in the nuclear region (Fig. 7, upper two panels). Use of pseudotyped particles labelled with MA.cherry/eGFP.Vpr in an identical experiment resulted in the opposite colour distribution, indicating that the relative distribution of the fluorescent proteins was determined by the viral fusion partners (data not shown). The diffuse cytoplasmic distribution we observed for the MA signal, which is in stark contrast to the pronounced membrane staining of target cells resulting from fusion of murine leukemia virus carrying a YFP-labelled envelope protein (Sherer et al., 2003), indicated that MA did not remain stably attached to the endosomal membrane after fusion had occurred. When bafilomycin A was added to block pH-mediated fusion, no separation of the red and green signals, but rather very similar distribution of intensities in both channels was detected (Fig. 7, lower two panels). In this case, very large double-coloured structures were found close to the nucleus, presumably representing particles trapped in endo-lysosomal structures. Accumulation of spatially separated bulk fluorescent signals was also not observed for particles lacking any viral surface protein and therefore incompetent for entry (data not shown). These data clearly indicate that a fusion-dependent separation of red and green signals does occur in our system. However, even when using efficiently fusing VSV-G pseudotyped particles, we did not visualize individual colour separation events. This may partly be explained by the strong double-coloured signals resulting from particles accumulated in endosomes, which would render detection of the weaker signal of individual fusion events difficult (see also below).

Role of heparan sulfate in particle immobilization and uptake

In the studies with HIV-1 envelope carrying particles described above, it became apparent that the large number of immobile complete particles accumulating at the cell surface presents a major obstacle for microscopic detection of single fusion events. Immobilization of complete particles was also observed, albeit at a lower frequency, when particles lacking the viral envelope protein were used (Fig. 8B and data not shown). This result indicated that an attachment factor different from the specific gp120–CD4 interaction contributed to this stable cell surface binding. Work from several laboratories has established that heparan sulfate – although not essential for HIV-1 entry – can play a role in the attachment of HIV-1 (Ugolini et al., 1999). This interaction has been reported to be of functional importance at least in some host cells (Bobardt et al., 2003; Zhang et al., 2002). Based on these results, we tested if heparan sulfate was responsible for the apparently non productive immobilization of double-labelled particles to HeLaP4 cells.

Cells were treated for 30 min with heparinase I to remove heparan sulfate from the cell surface and the efficacy of treatment was confirmed by flow cytometry using an anti-heparan sulfate antibody (data not shown). Since previously published studies investigated the effect of heparinase treatment on virus attachment by binding at low temperature, we first incubated heparinase-treated as well as mock-treated cells with fluorescent particles for 30 min on ice. Subsequently, the amount of bound fluorescence was quantitated by flow cytometry. Fig. 8A shows that fluorescent particle binding to cells was reduced to undetectable levels in heparinase-treated cells, indicating that heparan sulfate serves as major attachment factor on these cells.

Next we analyzed the effect of heparinase treatment on fluorescent particle immobilization under live cell imaging conditions (Fig. 8B). As observed in the previous experiments,

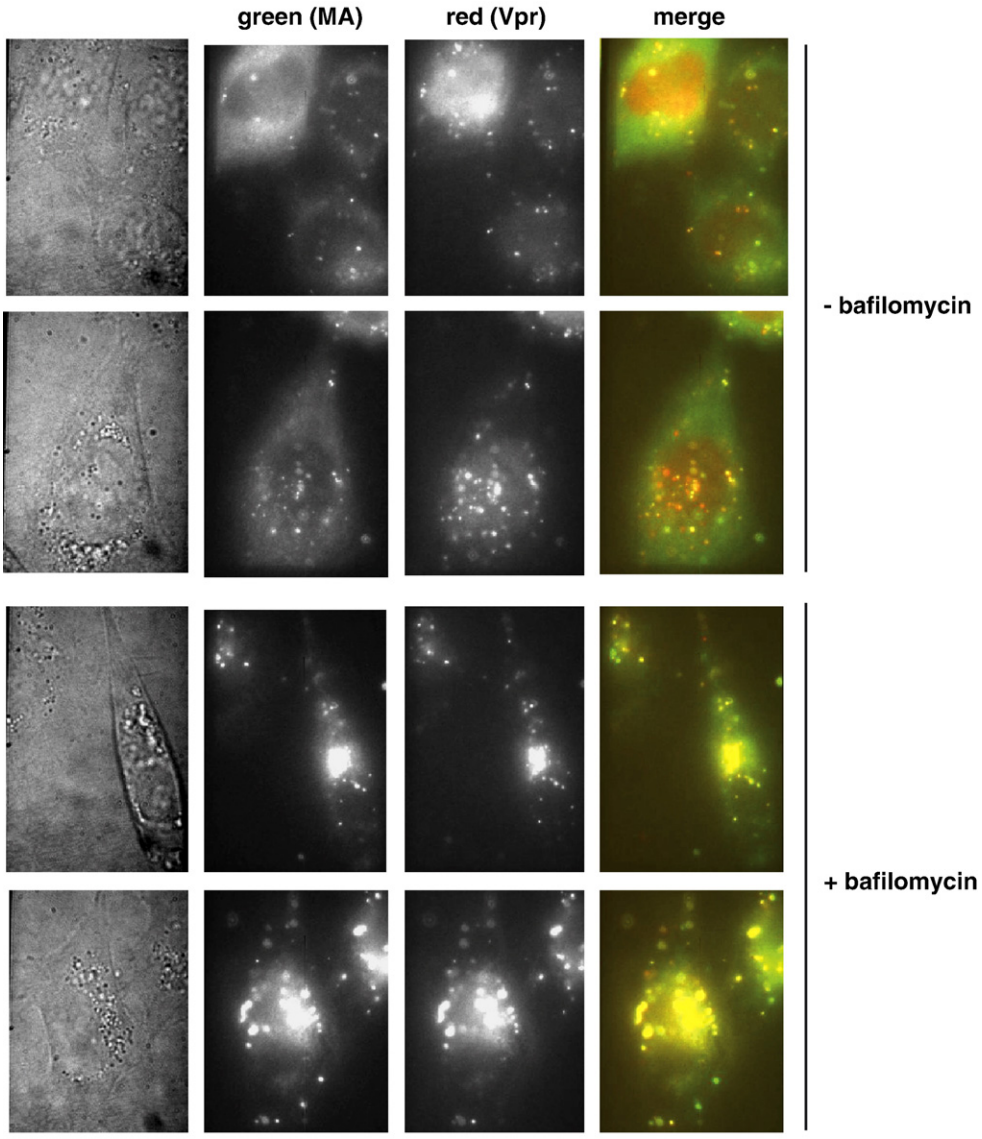

Fig. 7. Intracellular separation of MA and Vpr attached signals upon entry of VSV-G pseudotyped VLPs. HeLaP4 cells were pre-incubated for 25 min in the presence or absence of 25 nM bafilomycin A as indicated. Subsequently MA.eGFP/mRFP.Vpr-labelled VLPs pseudotyped with VSV-G protein were added and incubation was continued at 37 °C. Images shown here were recorded approximately 2 h after addition of virus as described under Materials and methods. Two images from the same experiment are shown for each condition.

incubation of virus with untreated or mock-treated control cells at 37 °C led to the accumulation of large numbers of immobilized dual-labelled particles at the cell surface. Concordant with the data obtained by flow cytometry (Fig. 8A), enzymatic removal of heparan sulfate from the cell surface strongly reduced the accumulation of immobile particles under live cell imaging conditions at 37 °C, while brief membrane contacts were still observed. Stable attachment of complete VLPs to heparinase-treated cells was slowly recovered upon prolonged incubation (>1 h after removal of heparinase), presumably due to newly synthesized heparan sulfate linked proteoglycans (data not shown). These results indicate that heparan sulfate can capture complete HIV-1 particles at the cell surface in an apparently non-productive way. Heparan sulfate also contributed to fluorescent particle endocytosis (Fig. 8C). While large amounts of double-labelled particles accumulated within untreated cells upon prolonged incubation (>20 min), only a few intracellular particles were detected in treated cells under the same conditions. It is currently not clear, however, whether this indicates that endocytosis is a consequence of prior membrane immobilization. While this is suggested by their common dependence on cell surface heparan sulfate, there are at least some particles that remain immobilized at the cell surface for several hours and may never be endocytosed.

To investigate whether abolishing particle immobilization affected productive HIV-1 infection, we determined the effect of heparinase treatment on infection. Previous studies of this kind have yielded different results, depending on the virus isolate, the source of virus, the host cell and the assay conditions used (Zhang et al., 2002 and references therein). For HeLa CD4 cells,

heparinase treatment has been reported to completely abolish HIV infection (Mondor et al., 1998) or to have no effect on HIV susceptibility (Ibrahim et al., 1999), respectively. To test for the effect of our treatment on productive infection, the HeLa-derived TZM reporter cell line (Wei et al., 2002) was incubated with heparinase as above and infected with wild-type HIV-1_{NL4-3}. Virus entry was blocked by treatment with the entry inhibitor AMD3100 after 30 min or 5.5 h, respectively, and infection was quantitated by measuring luciferase activity in cell extracts at 48 h after virus addition. Parallel infection experiments were carried out in DMEM or in PBS supplemented with Mg^{2+} and Ca^{2+}, respectively, because the latter had been used in imaging experiments. As shown in Fig. 8D, productive infection was reduced approximately 2.5-fold, but clearly not abolished by

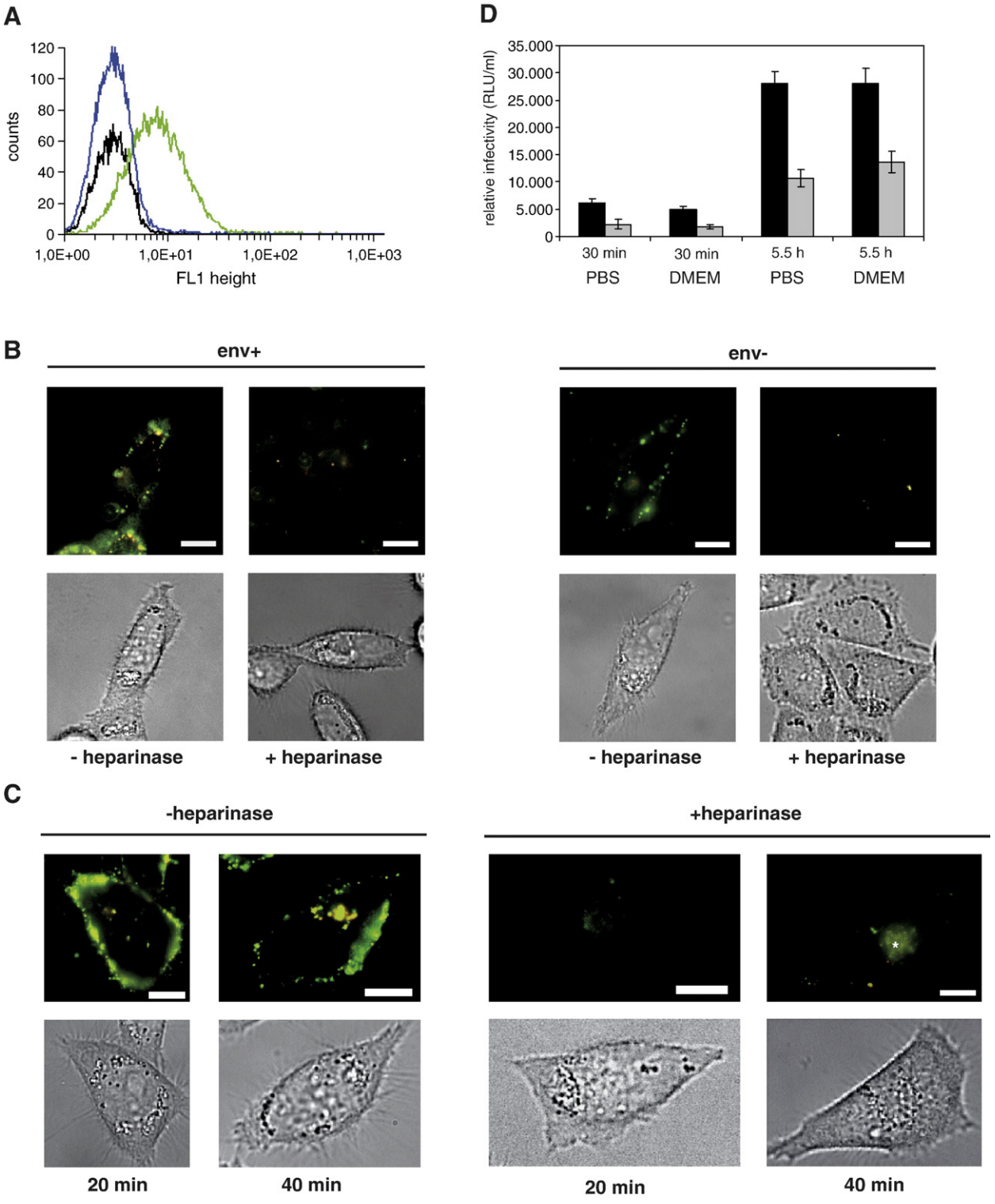

heparinase treatment. While the overall infection rate was lower when virus fusion was blocked after 30 min, the relative effect of treatment was very similar for both entry times tested. Replacement of DMEM by supplemented PBS during infection had no effect.

These experiments revealed that heparinase treatment only moderately decreased HIV-1 infection, while almost completely abolishing immobilization of complete particles at the plasma membrane. This result supports the hypothesis that the majority of immobilized particles represent products of non-productive interaction. We speculate that the heparinase-mediated reduction in infectivity can be explained, at least in part, by the decreased endosomal uptake following heparinase treatment (compare Fig. 8C). We had previously shown that inhibition of clathrin-dependent endocytosis decreased productive HIV infection in a HeLaP4-derived cell line by 40–90% (Daecke et al., 2005). In summary, removal of heparan sulfate from the cell surface provides improved conditions for live cell imaging of entry kinetics since accumulation of double-labelled particles at the cell surface is virtually abolished and endocytosis of complete particles is strongly reduced, while virus entry by fusion at the plasma membrane can still occur.

In this report, we have generated and characterized that dual fluorescent HIV-1 derivatives, which display a high degree of double labelling, are fully entry competent and are well suited to study cell interaction of single particles with high time resolution. Optimal conditions for the observation of single virus–cell interactions at the plasma membrane with high time resolution were established and removal of cell surface heparan sulfate was found to be important to avoid obscuring fusion events by immobilized complete particles. As outlined above, we expect that membrane fusion should be indicated by the spatial separation of the eGFP and mRFP signals from one particle. Whereas we could follow a large number of the different types of virus–cell interactions summarized in Fig. 6, clear colour separation events at the plasma membrane were not apparent in several hundred particle traces analyzed in the initial imaging experiments, suggesting that HIV fusion at the plasma membrane occurs only rarely in comparison to the brief membrane touches, particle immobilization and endocytosed particles observed. When fusion efficiency was enhanced by the use of VSV-G pseudotyped VLPs, increasing bulk separation of colours over time clearly indicated that fusion, followed by separation of MA and CA did occur. The reason why no individual fusion events were observed in this case is presently unclear. It is possible that the frequency of events was still too low to capture events in single cells during the necessarily short observation periods of the real-time measurements. Additionally, while McDonald et al. (2002) have shown that fluorescently labelled Vpr can be used to microscopically follow subviral complexes within the cell, we cannot exclude that a proportion of the incorporated mRFP.Vpr protein does not stay attached with the viral core, which would result in a concomitant decrease of signal intensity in both channels upon fusion. Furthermore, although it is generally believed that the majority of virion-associated MA molecules is not part of the subviral complex trafficking to the nucleus, it cannot be ruled out at present that the separation of the MA layer from the viral core is incomplete at the time of fusion. While our data clearly indicate that MA does not stay attached to the membrane after fusion, definition of the precise stages of entry will likely only be possible using automated quantitative analyses of movements and changes in relative colour distribution over time of individual particles from a large number of movies. Combining the entry competent double-labelled virions described here with automated tracking of many individual events should thus provide us with a powerful tool for investigating the entry pathway of HIV.

Materials and methods

Plasmids

The infectious HIV-1 proviral plasmid pNLC4-3 and its fluorescently labelled derivative have been described previously (Bohne and Kräusslich, 2004; Müller et al., 2004). Plasmids pCHIV and pCHIV.eGFP were constructed by cloning an *Xho*I–*Xba*I fragment comprising the complete HIV-derived sequence from pKHIV and pKHIV.eGFP (Müller et al., 2004), respectively, into pcDNA3.1(Zeo)-(Stratagene). Plasmids pCHIV (Env-) and pCHIV(Env-) were constructed from their wt env counterparts by exchange of an *Age*I–*Xho*I fragment with the corresponding fragment from subviral plasmid PA3, in which the *Nde*I site at nt 6401 of the NL4-3 proviral sequence was filled in with Klenow polymerase to generate a frameshift in the *env* gene. Plasmid pmRFP.Vpr was constructed from peGFP-Vpr (McDonald et al., 2002) by excising the eGFP open reading frame using *Nhe*I and *Sca*I and replacing it with a *Nhe*I–*Sca*I PCR fragment encoding the mRFP1 open reading frame amplified from plasmid pRSET-mRFP1 (Campbell et al., 2002).

Fig. 8. Effects of heparinase treatment on VLP immobilization and cell infectability. (A) Effect on VLP attachment as determined by flow cytometry. Following heparinase treatment, HeLaP4 cells were incubated with fluorescently labelled VLPs for 30 min on ice and the particle-associated eGFP fluorescence was determined by flow cytometry as described in Materials and methods. Blue line: autofluorescence of cells; green line: mock-treated cells; black line: heparinase-treated cells. (B) Effect on VLP immobilization as visualized in live cell imaging experiments. Heparinase-treated or mock-treated HeLaP4 cells were incubated with VLPs carrying HIV-1 Env proteins or an Env(−) variant, respectively, at 37 °C and monitored under conditions used for live cell imaging as described in Materials and methods. Images shown here were recorded 45 min after addition of particles. Fifty consecutive frames each (5 s in total) were averaged to dispose of signals resulting from diffusing particles in solution. (C) Reduction of particle endocytosis after removal of heparan sulfate by heparinase from the surface of HeLaP4 cells. Data shown here were recorded 20 min and 40 min post-addition of Env(+) VLPs, respectively, as described for Fig. 8B. Cellular autofluorescence in the nuclear region in one of the images is marked (*). Scale bar: 10 μm. The corresponding movies are provided as supplementary material. (D) Effect on cell infectability. Following heparinase treatment for 30 min, treated (grey bars) or mock-treated (black bars) HeLa TZM cells were incubated with HIV-1_{NL4-3} corresponding to 50 ng p24/well for the indicated times and infection was scored by measuring the activity of the Tat-dependent luciferase reporter protein as described in Materials and methods. Measurements were carried out in triplicate. One representative out of three independent experiments is shown.

Antisera

Polyclonal rabbit antisera were raised against purified recombinant MA protein or a synthetic full-length Vpr peptide, respectively. Rabbit antiserum raised against gp120 was kindly provided by V. Bosch (DKFZ, Heidelberg).

Tissue culture

293T cells, HeLaP4 cells and TZM reporter cells (Wei et al., 2002) were kept in Dulbecco's modified Eagle's medium (DMEM), supplemented with 10% fetal calf serum, penicillin, streptomycin and glutamine. Cells destined to be used in live cell imaging were cultivated in HybridoMed 1000F medium (Biochrom). Imaging was performed in PBS supplemented with 1 mM $CaCl_2$ and 0.5 mM $MgCl_2$.

Preparation of labelled particles

293T cells were transfected with a mixture of unlabelled and eGFP-labelled HIV-1-derived plasmids (pNLC4-3, pCHIV and derivatives) and pmRFP.Vpr at the indicated molar ratio by calcium phosphate precipitation. For generation of VSV-G pseudotyped particles, cells were transfected with a plasmid expressing VSV-G protein (Emi et al., 1991) together with pCHIV(Env-), pCHIV.eGFP(Env-) and pmRFP.Vpr. At 44 h post-transfection (hpt), medium was harvested and cleared by filtration through a 0.45-μm filter. Particles were concentrated by ultracentrifugation through a 20% (w/w) sucrose cushion. Particles were resuspended at 3.3 μl/ml culture supernatant in ice-cold phosphate-buffered saline (PBS) supplemented with 10% fetal calf serum and 10 mM HEPES pH 7.3, rapidly frozen in liquid nitrogen and stored at −80 °C. The particle concentration was quantified by p24 ELISA. To determine the relative fluorescence intensity of particle preparations, emission spectra were recorded at excitation wavelengths of 488 nm (eGFP) or 584 nm (mRFP), respectively, using an SLM Aminco spectrofluorometer.

Infection of TZM reporter cells

The infectivity assays were performed in a 96-well plate format. 5×10^3 TZM cells per well were plated and infections were carried out on the following day adding cleared and filtered medium from 293T producer cells, transfected with the indicated plasmids. After 48 h, cells were lysed and HIV Tat driven luciferase activity was measured using the Steady-Glo-Assay (Promega) according to the manufacturer's recommendations.

For evaluation of the effect of heparinase treatment, cells were seeded as before. After 24 h, the medium was removed and 100 μl PBS containing 2 U of heparinase I (Sigma) were added. Following 30 min of incubation at 37 °C, the heparinase solution was removed. Sucrose pelleted NL4.3 virus (amount equivalent to 50 ng CA determined by p24 ELISA) was diluted in PBS supplemented with 1 mM $CaCl_2$ and 0.5 mM $MgCl_2$,or DMEM/10%FCS and the cells were incubated with the virus dilution for the indicated times at 37 °C. Subsequently, virus was removed and DMEM containing 10 ng/ml AMD3100 (obtained through the NIH AIDS Research and Reference Reagent Program) was added to prevent further infection. At 18 h post-infection, 10 μM AZT (Sigma) was added to prevent second round infections. On the following day, medium was removed and luciferase reporter gene activity was quantified as above.

Beta-lactamase fusion assay

Particles carrying a Vpr-β-lactamase (Vpr.BlaM) fusion protein were obtained by co-transfection of 293T cells with pCHIV or an equimolar mixture of pCHIV and pCHIV.eGFP, respectively, and plasmid pMM310 (Münk et al., 2002) encoding the Vpr.BlaM fusion protein (5 μg pMM310: 15 μg pCHIV). Particles were harvested from the tissue culture supernatant at 44 hpt, concentrated by centrifugation through a sucrose cushion and their concentration was determined by p24 ELISA after heating for 10 min in 1% SDS. HeLaP4 cells (4×10^4 cells/well) were incubated in a 96-well plate (Costar #3603) with serial dilutions in 100 μl DMEM/10% FCS for 3.5 h at 37 °C. Subsequently, virus was removed, cells were washed once with CO_2-independent medium (Invitrogen), 70 μl of CCF2 β-lactamase loading solution (Invitrogen; prepared according to the manufacturer's instructions) was added and incubation was continued for 12 h at room temperature. Cells were washed with PBS, fixed with 3% paraformaldehyde and relative fluorescence intensities (excitation wavelength 409 nm, emission wavelengths 447 nm and 512 nm) were recorded using a TECAN Safire instrument. After subtraction of background from unstained cells at the respective emission wavelength, the ratio of emission intensities at 447/512 nm was calculated. The ratio obtained from mock-infected CCF2 stained cells was subtracted as background from all values obtained in the presence of virus.

Flow cytometry

Virus binding assays were performed using fluorescently labelled particles (60 ng p24 per 10^6 cells). Cells were harvested in PBS containing 0.7 mM EDTA, incubated with labelled particles for 30 min on ice, washed and subjected to flow cytometry using a FACSCalibur instrument and CellQuestPro software (Becton Dickinson). Bound virus was quantified by determining eGFP mean fluorescence. For heparinase treatment, cells were incubated with 2 U of heparinase I (Sigma) in 100 μl PBS for 30 min at 37 °C and washed twice with ice-cold PBS before virus addition. The efficiency of heparinase treatment was controlled by flow cytometry using a murine FITC-labelled monoclonal anti-heparan sulfate antibody (Clone 10E4, Seikagaku). After heparinase or mock treatment, the cells were washed and incubated with 100 μl of a 1:20 dilution of the antibody in PBS for 30 min on ice, subsequently washed and analyzed.

Live cell microscopy

For live cell fluorescence microscopy, cells were seeded at a density of 1×10^4 cells per well on chambered cover glass (Lab-

Tek, Nunc, #155411), precoated with collagen (Biochrom). After overnight incubation at 37 °C, medium was removed and fluorescently labelled virus, diluted in PBS supplemented with 0.5 mM $MgCl_2$ and 1 mM $CaCl_2$ was added. For imaging, we used a highly sensitive wide field setup (Visitron Systems) based on a Zeiss Axiovert 200 M microscope equipped with a back illuminated EM-CCD Camera (Cascade II, Roper Scientific) and an xyz-motorized stage (Applied Scientific Instrumentation). All experiments were performed at 37 °C using a microscope incubator chamber (EMBLEM, Heidelberg, Germany). Bright light images of cells were collected before they were observed by fluorescence microscopy. For excitation of the fluorophores, a Lambda DG4 light source (Sutter Instrument) was used, which allowed fast alternating excitation with appropriate single band filters for eGFP and mRFP1 (Chroma), respectively. The dual band eGFP/mRFP emission filter (Chroma) displayed no crosstalk under the imaging conditions used. Image acquisition and microscope control were performed with Metamorph (Universal imaging, Visitron). Images were recorded using the 16-bit range of the EMCCD camera with maximum amplification of the fluorescence signal, resulting in 65,536 grey values or relative intensity units (IU). In a typical data set, the offset in the GFP/RFP-channel was 5000/4200 IU and the mean intensity of noise was 9000/7100 IU with a standard deviation of 1500/1000 IU. VLP-derived signals were clustering between 11,000/9000 and 15,000/11,500 IU, with maximal signal intensities reaching 42,000/26,000 IU. VLPs were tracked by hand using the manual tracking feature of Metamorph.

For the experiments with VSV-G pseudotyped VLPs, cells seeded on the previous day were pre-incubated for 25 min in PBS supplemented with 0.5 mM $MgCl_2$/1 mM $CaCl_2$ in the presence or absence of bafilomycin A1 (Calbiochem; final concentration 25 nM) at 37 °C. Subsequently, virus was added and incubation was continued for 2 h at 37 °C. Data were recorded using a custom built microscope (Endress et al., manuscript in preparation) under comparable imaging conditions than those used in the other experiments. A pair of images was collected every 100 ms, one in each colour channel, focussing through a section in the middle of the cell. Frames number 6–10 from the respective channel were averaged and colour merged with identical display levels for all images and both colours, to generate the images shown in Fig. 7.

Determination of double labelling efficiency

Fluorescent particles were diluted in PBS and adhered to a glass coverslip. After focussing on the particles, the field of view was shifted to a neighboring area to record unbleached particles. To compensate for small focus differences, a z-stack with 0.1 μm spacing was recorded for both colours and the sharpest image of each colour was selected. Images were analyzed using ImageJ (http://rsv.info.nih.gov/ij/). Individual particles were identified visually in either the red or green channel, and the centres of the particles were marked. The intensity of the signal in each channel was defined as the integrated density within a circle of five pixel radius centered at the marked point. A minimum of 500 particles per preparation was measured. Background was calculated as the mean of a minimum of 100 equivalent measurements taken at positions where no particle was visible. A particle was considered as single labelled if the intensity in one channel was below one standard deviation of the mean background fluorescence from that channel.

Acknowledgments

We thank Maria Anders and Monika Franke for expert technical assistance. We gratefully acknowledge the generous gift of plasmids peGFP-Vpr by Tom Hope (University of Illinois, Chicago), pRSET-mRFP1 by Roger Tsien (University of California, San Diego) and pMM310 by Ned Landau (Salk Institute, La Jolla), and of antiserum against gp120 by Valerie Bosch (DKFZ Heidelberg).

This work was supported by the Deutsche Forschungsgemeinschaft (grant KR906/4-1 to BM and HGK and BR1027/16-2 to CB). JAGB was supported by fellowships from the Alexander von Humboldt Foundation and EMBO.

Appendix A. Supplementary data

Supplementary data associated with this article can be found, in the online version, at doi:10.1016/j.virol.2006.10.005.

References

Bobardt, M.D., Saphire, A.C., Hung, H.C., Yu, X., Van der Schueren, B., Zhang, Z., David, G., Gallay, P.A., 2003. Syndecan captures, protects, and transmits HIV to T lymphocytes. Immunity 18 (1), 27–39.

Bohne, J., Kräusslich, H.G., 2004. Mutation of the major 5′ splice site renders a CMV-driven HIV-1 proviral clone Tat-dependent: connections between transcription and splicing. FEBS Lett. 563, 113–118.

Bräuchle, C., Seisenberger, G., Endress, T., Ried, M.U., Buning, H., Hallek, M., 2002. Single virus tracing: visualization of the infection pathway of a virus into a living cell. ChemPhysChem 3 (3), 299–303.

Briggs, J.A., Wilk, T., Welker, R., Kräusslich, H.G., Fuller, S.D., 2003. Structural organization of authentic, mature HIV-1 virions and cores. EMBO J. 22 (7), 1707–1715.

Briggs, J.A., Simon, M.N., Gross, I., Kräusslich, H.G., Fuller, S.D., Vogt, V.M., Johnson, M.C., 2004. The stoichiometry of Gag protein in HIV-1. Nat. Struct. Mol. Biol. 11 (7), 672–675.

Campbell, R.E., Tour, O., Palmer, A.E., Steinbach, P.A., Baird, G.S., Zacharias, D.A., Tsien, R.Y., 2002. A monomeric red fluorescent protein. Proc. Natl. Acad. Sci. U.S.A. 99 (12), 7877–7882.

Cavrois, M., De Noronha, C., Greene, W.C., 2002. A sensitive and specific enzyme-based assay detecting HIV-1 virion fusion in primary T lymphocytes. Nat. Biotechnol. 20 (11), 1151–1154.

Daecke, J., Fackler, O.T., Dittmar, M.T., Kräusslich, H.G., 2005. Involvement of clathrin-mediated endocytosis in human immunodeficiency virus type 1 entry. J. Virol. 79 (3), 1581–1594.

Damm, E.M., Pelkmans, L., Kartenbeck, J., Mezzacasa, A., Kurzchalia, T., Helenius, A., 2005. Clathrin- and caveolin-1-independent endocytosis: entry of simian virus 40 into cells devoid of caveolae. J. Cell Biol. 168 (3), 477–488.

Eckert, D.M., Kim, P.S., 2001. Mechanisms of viral membrane fusion and its inhibition. Annu. Rev. Biochem. 70, 777–810.

Emi, N., Friedmann, T., Yee, J.K., 1991. Pseudotype formation of murine leukemia virus with the G protein of vesicular stomatitis virus. J. Virol. 65 (3), 1202–1207.

Ewers, H., Smith, A.E., Sbalzarini, I.F., Lilie, H., Koumoutsakos, P., Helenius, A., 2005. Single-particle tracking of murine polyoma virus-like particles on live cells and artificial membranes. Proc. Natl. Acad. Sci. U.S.A. 102 (42), 15110–15115.

Finke, S., Brzozka, K., Conzelmann, K.K., 2004. Tracking fluorescence-labeled rabies virus: enhanced green fluorescent protein-tagged phosphoprotein P supports virus gene expression and formation of infectious particles. J. Virol. 78 (22), 12333–12343.

Gallo, S.A., Finnegan, C.M., Viard, M., Raviv, Y., Dimitrov, A., Rawat, S.S., Puri, A., Durell, S., Blumenthal, R., 2003. The HIV Env-mediated fusion reaction. Biochim. Biophys. Acta 1614 (1), 36–50.

Ibrahim, J., Griffin, P., Coombe, D.R., Rider, C.C., James, W., 1999. Cell-surface heparan sulfate facilitates human immunodeficiency virus Type 1 entry into some cell lines but not primary lymphocytes. Virus Res. 60 (2), 159–169.

Lakadamyali, M., Rust, M.J., Babcock, H.P., Zhuang, X., 2003. Visualizing infection of individual influenza viruses. Proc. Natl. Acad. Sci. U.S.A. 100 (16), 9280–9285.

Lehmann, M.J., Sherer, N.M., Marks, C.B., Pypaert, M., Mothes, W., 2005. Actin- and myosin-driven movement of viruses along filopodia precedes their entry into cells. J. Cell Biol. 170 (2), 317–325.

Markosyan, R.M., Cohen, F.S., Melikyan, G.B., 2005. Time-resolved imaging of HIV-1 Env-mediated lipid and content mixing between a single virion and cell membrane. Mol. Biol. Cell 16 (12), 5502–5513.

Matlin, K.S., Reggio, H., Helenius, A., Simons, K., 1982. Pathway of vesicular stomatitis virus entry leading to infection. J. Mol. Biol. 156, 609–631.

McDonald, D., Vodicka, M.A., Lucero, G., Svitkina, T.M., Borisy, G.G., Emerman, M., Hope, T.J., 2002. Visualization of the intracellular behavior of HIV in living cells. J. Cell Biol. 159 (3), 441–452.

Mondor, I., Ugolini, S., Sattentau, Q.J., 1998. Human immunodeficiency virus type 1 attachment to HeLa CD4 cells is CD4 independent and gp120 dependent and requires cell surface heparans. J. Virol. 72 (5), 3623–3634.

Müller, B., Tessmer, U., Schubert, U., Kräusslich, H.G., 2000. Human immunodeficiency virus type 1 Vpr protein is incorporated into the virion in significantly smaller amounts than gag and is phosphorylated in infected cells. J. Virol. 74 (20), 9727–9731.

Müller, B., Daecke, J., Fackler, O.T., Dittmar, M.T., Zentgraf, H., Kräusslich, H. G., 2004. Construction and characterization of a fluorescently labeled infectious human immunodeficiency virus type 1 derivative. J. Virol. 78 (19), 10803–10813.

Münk, C., Brandt, S.M., Lucero, G., Landau, N.R., 2002. A dominant block to HIV-1 replication at reverse transcription in simian cells. Proc. Natl. Acad. Sci. U.S.A. 99 (21), 13843–13848.

Palokangas, H., Metsikko, K., Vaananen, K., 1994. Active vacuolar H+ATPase is required for both endocytic and exocytic processes during viral infection of BHK-21 cells. J. Biol. Chem. 269 (26), 17577–17585.

Platt, E.J., Wehrly, K., Kuhmann, S.E., Chesebro, B., Kabat, D., 1998. Effects of CCR5 and CD4 cell surface concentrations on infections by macrophagetropic isolates of human immunodeficiency virus type 1. J. Virol. 72, 2855–2864.

Raviv, Y., Viard, M., Bess Jr., J., Blumenthal, R., 2002. Quantitative measurement of fusion of HIV-1 and SIV with cultured cells using photosensitized labeling. Virology 293 (2), 243–251.

Rust, M.J., Lakadamyali, M., Zhang, F., Zhuang, X., 2004. Assembly of endocytic machinery around individual influenza viruses during viral entry. Nat. Struct. Mol. Biol. 11 (6), 567–573.

Seisenberger, G., Ried, M.U., Endress, T., Buning, H., Hallek, M., Bräuchle, C., 2001. Real-time single-molecule imaging of the infection pathway of an adeno-associated virus. Science 294 (5548), 1929–1932.

Sieczkarski, S.B., Whittaker, G.R., 2005. Viral entry. Curr. Top. Microbiol. Immunol. 285, 1–23.

Sherer, N.M., Lehmann, M.J., Jimenez-Soto, L.F., Ingmundson, A., Horner, S.M., Cicchetti, G., Allen, P.G., Pypaert, M., Cunningham, J.M., Mothes, W.R., 2003. Visualization of retroviral replication in living cells reveals budding into multivesicular bodies. Traffic 4 (11), 785–801.

Suomalainen, M., Nakano, M.Y., Keller, S., Boucke, K., Stidwill, R.P., Greber, U.F., 1999. Microtubule-dependent plus- and minus end-directed motilities are competing processes for nuclear targeting of adenovirus. J. Cell Biol. 144 (4), 657–672.

Ugolini, S., Mondor, I., Sattentau, Q.J., 1999. HIV-1 attachment: another look. Trends Microbiol. 7 (4), 144–149.

Wei, X., Decker, J.M., Liu, H., Zhang, Z., Arani, R.B., Kilby, J.M., Saag, M.S., Wu, X., Shaw, G.M., Kappes, J.C., 2002. Emergence of resistant human immunodeficiency virus type 1 in patients receiving fusion inhibitor (T-20) monotherapy. Antimicrob. Agents Chemother. 46 (6), 1896–1905.

Wilk, T., Gross, I., Gowen, B.E., Rutten, T., de Haas, F., Welker, R., Kräusslich, H.G., Boulanger, P., Fuller, S.D., 2001. Organization of immature human immunodeficiency virus type 1. J. Virol. 75 (2), 759–771.

Zhang, Y.J., Hatziioannou, T., Zang, T., Braaten, D., Luban, J., Goff, S.P., Bieniasz, P.D., 2002. Envelope-dependent, cyclophilin-independent effects of glycosaminoglycans on human immunodeficiency virus type 1 attachment and infection. J. Virol. 76 (12), 6332–6343.